25 Gb/s directly modulated ground-state operation of 1.3 μm InAs/GaAs quantum dot lasers up to 75°C

Zhongkai Zhang (张中恺)[1,2], Zunren Lü (吕尊仁)[1,2,*], Xiaoguang Yang (杨晓光)[1,2], Hongyu Chai (柴宏宇)[1,2], Lei Meng (孟 磊)[1,2], and Tao Yang (杨 涛)[1,2,]**

[1]*Key Laboratory of Semiconductor Materials Science, Institute of Semiconductors, Chinese Academy of Sciences, Beijing 100083, China*

[2]*Center of Materials Science and Optoelectronics Engineering, University of Chinese Academy of Sciences, Beijing 100049, China*

**Corresponding author: lvzunren@semi.ac.cn; **corresponding author: tyang@semi.ac.cn*

Received December 31, 2019; accepted March 25, 2020; posted online May 22, 2020

We report 25 Gb/s high-speed directly modulated ground-state operation of 1.3 μm InAs/GaAs quantum dot (QD) lasers grown by molecular beam epitaxy. The active region of the lasers consists of eight layers of p-doped InAs QDs with high uniformity and density. Ridge-waveguide lasers with a 3-μm-wide and 300-μm-long cavity show a low threshold current of 14.4 mA at 20°C and high temperature stability with a high characteristic temperature of 1208 K between 20°C and 70°C. Dynamic response measurements demonstrate that the laser has a 3 dB bandwidth of 7.7 GHz at 20°C and clearly opened eye diagrams even at high temperatures up to 75°C under a 25 Gb/s direct modulation rate.

Keywords: semiconductor lasers; quantum dot; molecular beam epitaxy; direct modulation.
doi: 10.3788/COL202018.071401.

Owing to the strong three-dimensional quantum confinement effect of carriers in quantum dots (QDs), InAs/GaAs QD lasers emitting at 1.3 μm have exhibited many superior characteristics over conventional quantum well counterparts, including low threshold current, high temperature stability, and high modulation speed[1–7]. This has made the InAs/GaAs QD lasers a very promising candidate for uncooled directly modulated light sources used in next generation low-cost, low-power-consumption, and high-speed fiber-optic communication systems. In order to realize these superior characteristics in real devices, the first challenge is to achieve a high-quality active region of multiple stacking layers of QDs with high density and high uniformity, which is very important to improve the maximum modal gain of the QD lasers[8]. The second one is to suppress the thermal escape of carriers at high temperatures, especially for the holes, whose energy level spacing is typically smaller than 10 meV[9]. So far, great efforts have been made to improve the material quality of InAs/GaAs QD lasers in order to achieve higher modal gain[10–12]. A p-type modulation doping technology was introduced to compensate the thermal escape of carriers, leading to a better thermal stability[9,13]. In 2010, Yang *et al.* reported the 10 Gb/s directly modulated operation up to 50°C of 1.3 μm InAs/GaAs QD lasers, whose active region consisted of only five stacked undoped QD layers[14]. Takada *et al.* reported ground-state 25 Gb/s operation of 1.3 μm p-doped InAs/GaAs QD lasers up to 70°C in 2012[15]. Subsequently, Arsenijević *et al.* reported the room-temperature (RT) 25 Gb/s operation of 1.3 μm InAs/GaAs QD lasers working at an excited state in 2014[16]. However, their eye diagrams showed obvious deterioration as the temperature increased, which was undesired for practical application.

In this Letter, we demonstrate the uncooled ground-state operation of 1.3 μm InAs/GaAs QD lasers under a direct modulation rate of 25 Gb/s at high temperatures up to 75°C. The QD lasers were grown by molecular beam epitaxy (MBE), and their active region consists of eight layers of InAs QDs with high density and high uniformity. Furthermore, p-type modulation doping was used to enhance the temperature stability of the devices. Ridge-waveguide lasers with a 3-μm-wide and 300-μm-long cavity were formed by standard lithography and dry etching, and one facet of the lasers was coated with a high-reflectivity (HR) of 95%. It is found that the ridge-waveguide laser has a low threshold current of 14.4 mA with a high slope efficiency of 0.46 W/A at 20°C, and it exhibits high temperature stability with a characteristic temperature (T_0) as high as 1208 K between 20°C and 70°C. Furthermore, the laser shows a 3 dB bandwidth of 7.7 GHz at 20°C and clearly opened eye diagrams with a dynamic extinction ratio (ER) of over 3 dB under a direct modulation rate of 25 Gb/s at the temperature range from 20°C to 75°C.

The InAs/GaAs QD laser structures used in this study were grown on a 2 inch (1 inch = 2.54 cm). Si-doped GaAs (100) substrate by MBE. Figure 1 schematically illustrates the laser structure. A 300 nm n-GaAs buffer layer was firstly deposited on the substrate, followed by a 1400 nm n-$Al_{0.4}Ga_{0.6}As$ lower cladding layer and an 85 nm undoped lower waveguide layer. Then, an active region consisting of eight layers of self-assembled InAs/GaAs QDs was deposited. Each InAs-QD layer has a thickness of 2.3 monolayers and is capped by a 4 nm $In_{0.18}Ga_{0.82}As$ strain-reducing layer and a subsequent 40 nm GaAs spacer layer. P-type modulation-doping technology was used to

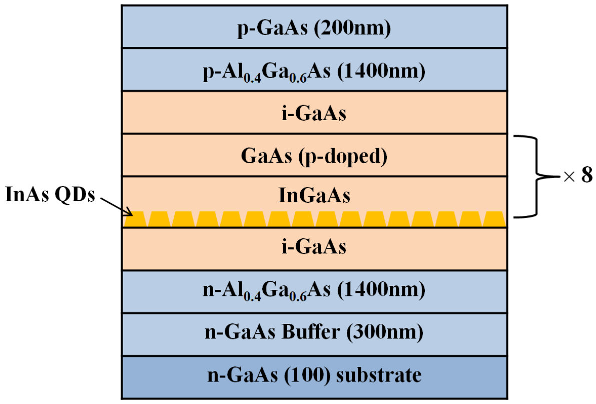

Fig. 1. Schematic diagram of the InAs/GaAs QD lasers.

improve the temperature stability and modulation characteristic of the QD lasers[8,11]. Finally, a 40 nm upper waveguide layer, a 1400 nm p-$Al_{0.4}Ga_{0.6}As$ upper cladding layer, and a 200 nm p-GaAs contact layer were deposited. Ridge-waveguide lasers with a 3-μm-wide and 300-μm-long cavity were fabricated with standard lithography and dry-etching technology, and then the back facet of the lasers was coated with an HR of 95%.

Figure 2 presents the RT photoluminescence (PL) spectra from single-layer and eight-layer InAs-QD samples with the same growth conditions as the laser. The inset in Fig. 2 shows the surface atomic force microscope (AFM) image of the eight-layer InAs-QD sample, in which the upper-most QDs layer was left uncapped for measurement. From the AFM measurement, the density of the InAs QDs for each layer is estimated to be about 4.5×10^{10} cm^{-2}. Furthermore, from the PL measurements, the full width at half-maximum of the PL spectra for the single-layer and eight-layer QD samples is 27.0 meV and 27.8 meV (nearly unchanged), respectively, and the peak intensity of the eight-layer QD sample is approximately 7.3 times stronger than that of the single-layer QD sample, showing that a high-quality QD active region with high uniformity and high density has been achieved.

Figure 3 shows the power-current (P–I) curves of the laser under CW injection, measured at the temperature range from 20°C to 70°C. From the measurement, the laser shows a threshold current of as low as 14.4 mA and a slope efficiency of as high as 0.46 W/A at 20°C, with an output power of over 20 mW. Moreover, as the temperature increases from 20°C to 70°C, the threshold current increases only from 14.4 mA to 14.9 mA. The inset in Fig. 3 plots the logarithmic threshold current of the laser as a function of temperature. From the inset, a T_0 of as high as 1208 K between the given temperature range can be obtained by fitting, showing the high temperature stability of the InAs/GaAs QD laser. This can be mainly ascribed to the high-performance active region of eight layers of p-doped InAs/GaAs QDs with the high uniformity and high density that we achieved. The saturation of the P-I curves at high temperatures as well as high injection levels can be mainly attributed to the heat accumulation, arising from insufficient heat dissipation of the measurement equipment at high temperatures.

Subsequently, small signal frequency response measurements for the lasers were carried out. The bias current was fixed at 50 mA. Figure 4 shows the small signal frequency responses at different temperatures of 20, 50, and 70°C. As shown in Fig. 4, a maximum 3 dB bandwidth of 7.7 GHz was observed at 20°C, and it decreased in sequence to 7 GHz and 6.3 GHz at 50 and 70°C, respectively. This decrease in bandwidth with the increase of temperature can also be attributed to the heat accumulation of the laser, which leads to enhanced thermal escape of carriers from QDs to barriers.

Finally, large signal response curves of the InAs/GaAs QD laser under a direct modulation rate of 25 Gb/s were

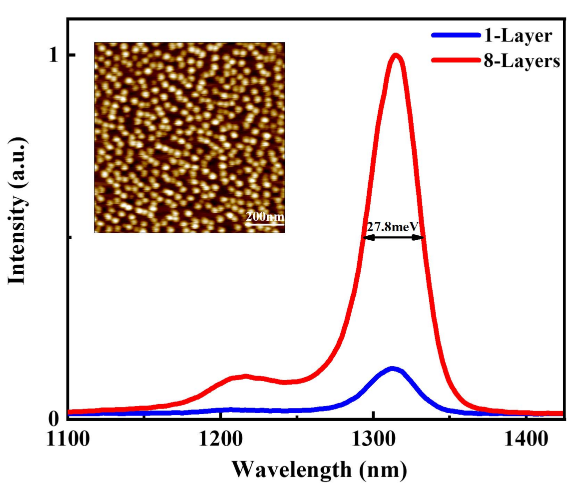

Fig. 2. PL spectra of the one-layer and the eight-layer QDs samples. The inset shows the surface AFM image of the surface QD layer for the eight-layer QD sample.

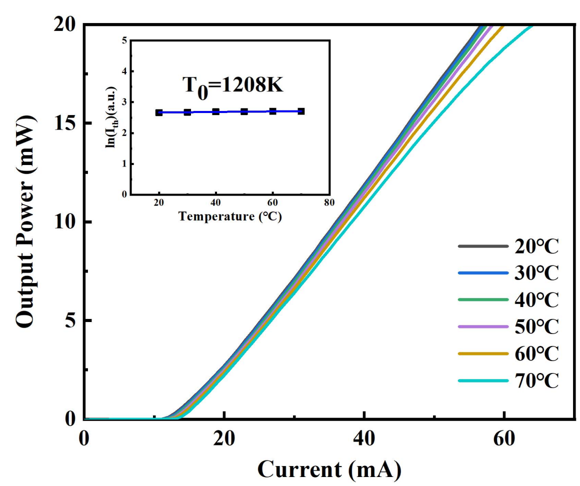

Fig. 3. P–I curves of the laser at different temperatures from 20°C to 70°C. The inset shows the logarithmic threshold current as a function of temperature.

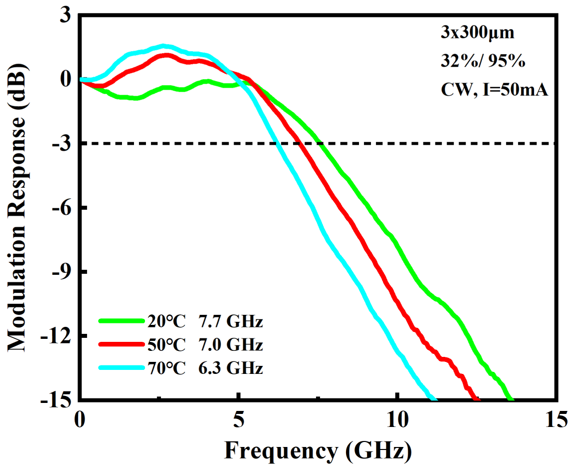

Fig. 4. Small signal frequency response curves of the InAs/GaAs QD laser, measured at different temperatures.

also investigated at different operation temperatures. The laser was also biased at 50 mA, and the peak-to-peak modulation amplitude was adjusted with the temperature to obtain the identical ER of about 3 dB. The laser was modulated by a 25 Gb/s non-return-to-zero (NRZ) pseudo-random binary sequence (PRBS) pattern with a code length of $2^{15}-1$, using SHF 12125B Serial BERT. A 25 Gb/s positive-intrinsic-negative (PIN) detector was used to receive the modulated optical signal, and the eye diagrams were captured by a sampling oscilloscope (Agilent 86100D). Figure 5 exhibits the 25 Gb/s eye diagrams of the InAs/GaAs QD laser operating at different temperatures of 20, 50, 70, and 75°C. Clearly opened eye diagrams were obtained at all of the given temperatures, and there was no obvious deterioration of the eye diagrams even at high temperatures up to 75°C, showing a great improvement compared with the results given in Refs. [14–16].

In summary, we have demonstrated uncooled ground-state operation of 1.3 μm InAs/GaAs QD lasers under a direct modulation rate of 25 Gb/s at high temperatures up to 75°C. The 3-μm-wide and 300-μm-long ridge-waveguide lasers exhibit a low threshold current of 14.4 mA and a high slope efficiency of 0.46 W/A at 20°C. Furthermore, the laser shows high temperature stability with a very high T_0 of 1208 K. Small signal frequency response measurements reveal that the laser has a 3 dB bandwidth of 7.7 GHz at 20°C. Large signal response measurements show that clearly opened eye diagrams under a direct modulation rate of 25 Gb/s for the laser can be observed at different temperatures from 20°C to 75°C. All the excellent results shown here can be attributed to the high-performance QD active region of eight layers of p-doped InAs/GaAs QDs with high uniformity and high density that we achieved, indicating the huge potential of the 1.3 μm InAs/GaAs QD lasers for uncooled directly modulated high-speed light sources used in next generation low-cost and low-power-consumption fiber-optic communication systems.

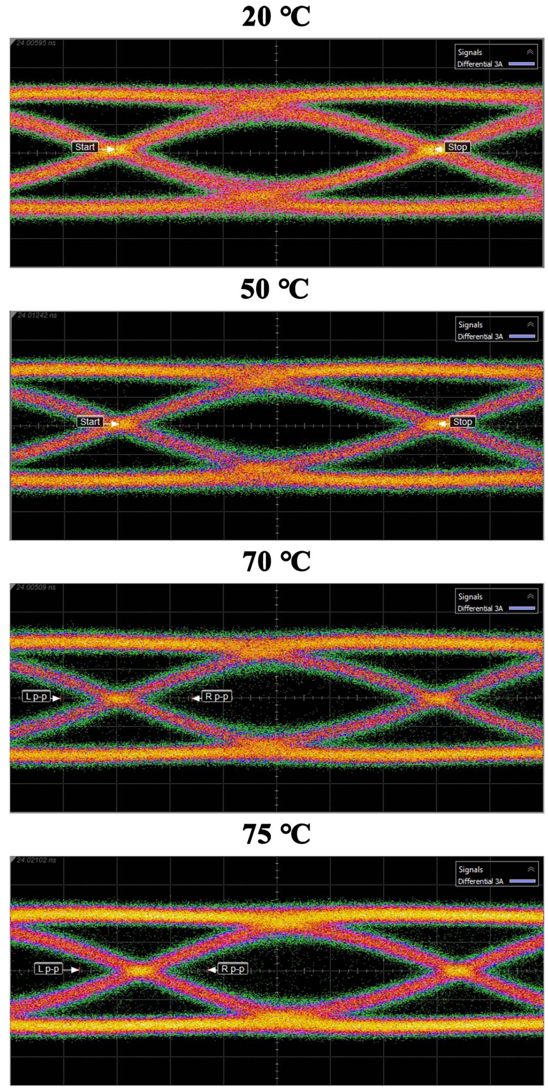

Fig. 5. Eye diagrams of the InAs/GaAs QD laser at different temperatures.

This work was supported by the National Key Research & Development (R&D) Program of China (No. 2016YFB0402302) and the National Natural Science Foundation of China (Nos. 91433206, 61574139, and 61841403). The authors would like to thank Mr. Yiming He and Prof. Dan Lu for beneficial discussions and great help in device characterizations.

References

1. Y. Arakawa and H. Sakaki, Appl. Phys. Lett. **40**, 939 (1982).
2. Y. Arakawa and A. Yariv, IEEE J. Quantum Electron. **22**, 1887 (1986).
3. H. Shimizu, S. Saravanan, J. Yoshida, S. Ibe, and N. Yokouchi, Jpn. J. Appl. Phys. **44**, L1103 (2005).
4. T. Kageyama, K. Nishi, M. Yamaguchi, R. Mochida, Y. Maeda, K. Takemasa, Y. Tanaka, T. Yamamoto, M. Sugawara, and Y. Arakawa, in *European Conference on Lasers and Electro-Optics* (2011), paper PDA_1.
5. S. Fathpour, Z. Mi, P. Bhattacharya, A. Kovsh, S. S. Mikhrin, I. L. Krestnikov, A. V. Kozhukhov, and N. N. Ledentsov, Appl. Phys. Lett. **85**, 5164 (2004).

6. L. V. Asryan and R. A. Suris, Appl. Phys. Lett. **96**, 221112 (2010).
7. Y. Arakawa, S. Iwamoto, S. Kako, M. Nomura, and D. Guimard, Chin. Opt. Lett. **6**, 718 (2008).
8. S. M. Kim, Y. Wang, M. Keever, and J. S. Harris, IEEE Photon. Technol. Lett. **16**, 377 (2004).
9. O. B. Shchekin and D. G. Deppe, Appl. Phys. Lett. **80**, 2758 (2002).
10. K. Otsubo, N. Hatori, M. Ishida, S. Okumura, T. Akiyama, Y. Nakata, H. Ebe, M. Sugawara, and Y. Arakawa, Jpn. J. Appl. Phys. **43**, L1124 (2004).
11. K. Takada, Y. Tanaka, T. Matsumoto, M. Ekawa, Y. Nakata, T. Yamamoto, M. Sugawara, and Y. Arakawa, in *Optical Fiber Communication Conference* (2009), paper JWA28.
12. Q. Han, Z. Niu, H. Ni, S. Zhang, X. Yang, Y. Du, C. Tong, H. Zhao, Y. Xu, H. Peng, and R. Wu, Chin. Opt. Lett. **4**, 413 (2006).
13. D. G. Deppe, H. Huang, and O. B. Shchekin, IEEE J. Quantum Electron. **38**, 1587 (2002).
14. H. M. Ji, T. Yang, Y. L. Gao, P. F. Xu, Y. X. Gu, Y. Liu, L. Xie, and Z. G. Wang, Chin. Phys. Lett. **27**, 034209 (2010).
15. M. Ishida, M. Matsuda, Y. Tanaka, K. Takada, M. Ekawa, T. Yamamoto, T. Kageyama, M. Yamaguchi, K. Nishi, M. Sugawara, and Y. Arakawa, in *Lasers and Electro-Optics* (2012), paper CM1I.2.
16. D. Arsenijević, A. Schliwa, H. Schmeckebier, M. Stubenrauch, M. Spiegelberg, D. Bimberg, V. Mikhelashvili, and G. Eisenstein, Appl. Phys. Lett. **104**, 181101 (2014).